Radhi et al., Mong. J. Chem., 25(52), 2024, 19-25
https://doi.org/10.5564/mjc.v25i52.3450

Using activated and modified adsorbent surfaces from banana peels to remove the green Janus dye: A kinetic, isothermal, and thermodynamic study

Israa Mohammed Radhi[1], Suha Sahab Abd[1], Russol Abdul Salam Faraj[1], Ahmed Mohammed Abbas[1*] and Takialdin A. Himdan[2]

[1]*College of Education for Pure Sciences (Ibn Al-haitham), University of Baghdad, Baghdad, Iraq*
[2]*College of Dentistry, Al-Esraa University, Baghdad, Iraq*

**Corresponding author: ahmed.m.a@ihcoedu.uobaghdad.edu.iq;* ORCID: https://orcid.org/0000-0002-2001-4704

Received: 04 June 2024; revised: 20 August 2024; accepted: 11 September 2024

ABSTRACT

In order for the process of removing pollutants, including dyes, from the aquatic environment to be effective, plant wastes such as banana peels were used as adsorbent surfaces by thermally activating them (ABP) and modifying them with iron oxide nanoparticles (MABP), which were characterized using Fourier transform infrared (FT-IR) and X-ray diffraction (XRD) techniques. They were applied in the field of Janus green (JG) dye adsorption for the batch system and studied the effect of several factors (adsorbent weight, contact time, initial concentration, and temperature). Their data were analyzed kinetically using first- and second-order kinetic models and they were found to follow the second order. Their data were also analyzed through the equilibrium isotherms (Freundlich and Langmuir), and it was found to follows the Freundlich isotherm model. The thermodynamic functions for the dye adsorption process on both surfaces were calculated, through these functions, it was found that the dye adsorption process is spontaneous, easy, regular, and exothermic.

Keywords: **Keywords:** *Banana peels, Thermal activation, Iron oxide NPs, Janus green, Adsorption*

INTRODUCTION

The increase in industrial activities and the rise in population at present represent multiple problems in our ecosystem due to the pollution resulting from these activities, which creates a threat to water safety [1]. The disposal of liquid industrial waste, whether treated or untreated, into water, is considered the main cause of pollution [2]. High levels of contaminated substances in drinking water or industrial water samples represent the acceptable level, which is then called contaminated or unsafe water [3]. Numerous industrial dyes and other organic and inorganic compounds that could be harmful to agriculture, public health, and other sectors are present in this water [4].Among these contaminants are dyes, which are artificially produced organic substances that attach to textile surfaces to impart colour [5]. Due to their low cost and resilience against heat and other variables, artificial dyes have become more popular in the textile industry than natural colours. As a result, these portion's liquid waste is dumped into the water, polluting it [6]. Dye-containing wastewater is challenging to treat because the dyes are refractory particles that are extremely resistant to oxidizing chemicals, and removing them can be costly [7]. As a result, adsorption can be employed in the removal process due to its high efficiency even at high dye solution concentrations, safety, and technological advancement over alternative approaches [8]. Additionally, dye from contaminated water can be removed using straight-forward adsorbents that have the capacity to hydrolyze [9].Banana peels are one of these materials. They have attracted the attention of many researchers because of their easy availability throughout the year and also because of the presence of many different functional groups that allow these peels to adsorb cationic and anionic materials from the surfaces of active sites [10]. Recently, the nanoscale form of metal oxides, including iron oxide, has been used in many applications, including treating water from pollutants such as heavy metals and dyes, due to their excellent surface properties and high effectiveness, which considers them promising adsorbent surfaces in the future [11-13]. The adsorption of different dyes using banana peels has been studied in many previous studies [14, 15]. Most of these studies shed light on the possibility of using banana peels to remove dyes from their standard solutions, as they showed high efficiency in removing them and were applied commercially due to their low economic cost [16]. They [17] studied the possibility of using banana peels to absorb Congo red dye from its aqueous solution by activating it with sodium hydroxide. While [18] studied the use of banana peel waste for the adsorption of methylene blue dye because it is an inexpensive and environmentally friendly material, the surface was modified using Rhizopus microorganisms, and the modified surface showed high efficiency in the adsorption of the dye. Therefore, this article aims to thermally activate banana peels modify them with iron oxide nanoparticles and characteize those using techniques (XRD and FT-IR) and application of the prepared surfaces in the field of Janus green dye adsorption from aqueous solution.

EXPERIMENTAL

Activation of banana peel surfaces (ABP): The banana peels used in this study were activated by washing and heating to a temperature of 200 °C in an oven (Daihan Labtech, Korea) for 1 hour and then grinding. The product (ABP) was diagnosed using the techniques of XRD and FT-IR (Shimadzu, Japan). ***Modification of activated banana peel surfaces (MABP):*** The activated banana peels were modified by taking 10 g of the activated substance and adding 1 g of ferrous sulfate heptahydrate (BDH chemicals, UK) with 0.4 g of sodium hydroxide (BDH chemicals, UK) and 100 ml of distilled water. The mixture was placed on the stirrer for 3 hs at a temperature of 50 °C. Then 100 ml of NaOH with a concentration of 0.1 M was prepared, added to the mixture, and placed in the sonicator for 1 h. After that, the prepared precipitate was washed and dried in an oven (Daihan Labtech, Korea) at 80 °C for 3 hs, and then ground. The product (MABP) was diagnosed using the techniques of XRD and FT-IR.

Adsorption tests: First, a number of experiments were conducted to adsorption of JG dye on banana peels without any treatment, but we did not obtain acceptable results. Second, adsorption experiments were conducted in this study using a batch system, where several factors were tested through experiments of taking different weights (0.01-0.07) g for both surfaces (ABP and MABP) by balance (Sartorius Lab, Germany) and over a range of time (15-90) min and a range of concentrations (10–35) mg/l of the Janus green B dye (JG) at a range of temperatures (25, 30, 35, 40) °C at pH 7 and particle size 75 μm using a shaking water bath (Labtech, Korea). The surface was separated from the JG dye solution using a centrifuge (Hettich, Germany), and the absorbance of the JG dye solution was measured using a UV-vis spectrophotometer (Shimadzu, Japan) at λ_{max} for the JG dye. The amount of adsorbed dye and the percentage of adsorption (% A) were calculated through the equations [19].

$$q_e = \frac{(C_\circ - C_t)V}{m} \quad (1)$$

$$\%A = \left(\frac{C_\circ - C_e}{C_\circ}\right) \times 100 \quad (2)$$

m- mass of (ABP and MABP) surfaces (g)
C_o- concentration of JG dye adsorbed (mg/L) at (0 and t_{eq})
V- volume of JG dye solution (L)

RESULTS AND DISCUSSION

Characterization of surfaces

XRD analysis: It can be observed from Fig.1. The XRD spectrum of thermally activated banana peels (ABP), where distinct and sharp peaks were found at (2θ: 28.5, 40.8°), and from Fig. 1 show the surface after modification (MABP), which includes (2θ: 31.7, 38.8, 44.6, 50.3, 55.5, 63.5, 73.8°) and corresponds to the levels of Miller indices (hkl): (311), (400), (422), (511), (440), and (533) respectively. These values correspond to the standard values for iron oxide nanoparticles according to the card (JCPDS file no. 65-3107). We used the Debye-Scherer equation to obtain the crystallite size [20]:

$$S_{hkl} = \frac{k\lambda}{b\cos\theta} \quad (3)$$

S_{hkl} - the average crystallite size (nm)
K - the Scherer constant (0.89)
λ - the incident X-ray wavelength
θ - the Bragg diffraction angle
b - the full width high maximum

The average crystallite sizes are 31, 24, and 26 nm for the ABP, Fe_2O_3 NPs, and MABP surfaces, respectively. Which indicate modifying banana peels with iron oxide nano particles [21].

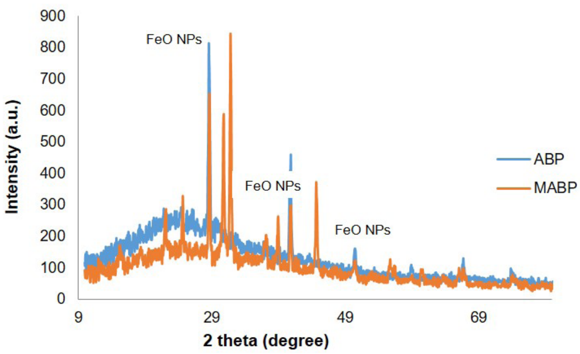

Fig. 1. XRD Graph of activated banana peel (ABP), modified and activated banana peel (MABP).

FT-IR analysis: Fig. 2 represents the FT-IR spectrum of thermally activated banana peels (ABP) at a temperature of 200 °C, which affected all the peaks in the spectrum.It is noted that there is a strong broad peak at 3375.4 cm^{-1} due to vibration stretching of the group hydroxyl group. Which belong to cellulose polymeric compounds or groups of amino acids, and the presence of two peaks at (2906.7 and 2829.5) cm^{-1}, which indicate the presence of symmetric and asymmetric stretching respectively of the (C-H) bonds of the alkanes, as well as the presence of a small peak at (1672.2) cm^{-1}, which indicates the presence of stretching bonds (C=O) that belong to carboxylic acids or esters, the presence of a peak at (1550.7) cm^{-1}, which indicates the presence of absorbed water molecules, the presence of a peak at (1367.5) cm^{-1}, which indicates the presence of a bend of the bond (C-H), the presence of a peak at (1089.7) cm^{-1}, which goes back to the (C-O) bond of the lignin compound, the presence of a peak at (725.2) cm^{-1}, which goes back to the bend of the bond for the amino groups. Also Fig. 2 show the FT-IR spectrum after modification (MABP) with iron particles, which led to relative changes in all the characteristic peaks before modification, new peak was also observed at 617 cm^{-1}, which is due to the stretching of Fe-O for iron oxide nanoparticles [22, 23].

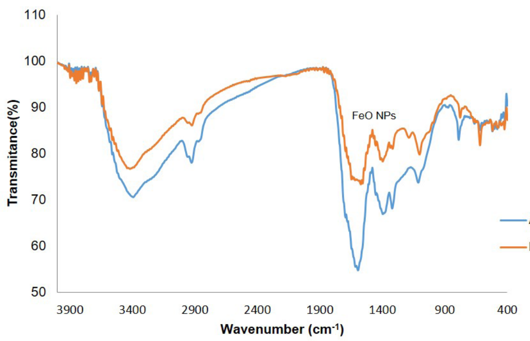

Fig. 2. FT-IR Graph of activated banana peel (ABP), modified and activated banana peel (ABP)

Adsorption studies

Effect of ABP and MABP adsorbent weights: The effect of ABP and MABP adsorbent doses on the adsorption of JG dye from an aqueous solution is presented in Fig. 3 shows that the highest amount of JG dye adsorption is at weight (0.01 g), but with increasing weight of the adsorbing surface, a decrease in the amount of adsorbed dye is noted, indicating an increase in the availability of adsorption sites not occupied by the adsorbed JG dye molecules, which causes a decrease in the amount of JG dye adsorbed for both surfaces. Therefore, for adsorbents (ABP and MABP), a dose of 0.01 g was chosen in this study due to its higher adsorption capacity [24].

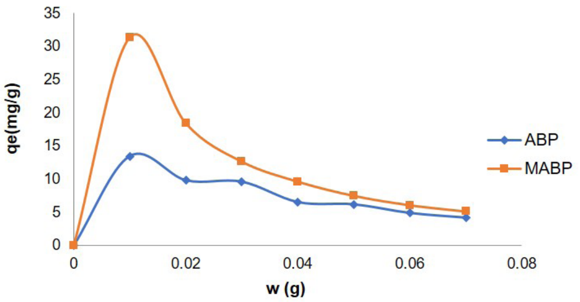

Fig. 3. Effect of ABP and MABP adsorbents weight on the adsorption of JG dye

Effect of contact time and temperature: The profile of the time-dependent study on the adsorption of JG dye onto ABP and MABP surfaces at different temperatures is shown in Figs. 4 and 5. The result showed that the removal rate of JG dye was rapid within the first 20 min, after which it a little increased, attaining equilibrium around 60 min, with 33% and 46% of JG dye removed by ABP and MABP surfaces, respectively. It is also noticeable that the percent of dye adsorption decreases with increasing temperature, which indicates that the JG dye adsorption process on both surfaces is exothermic [25].

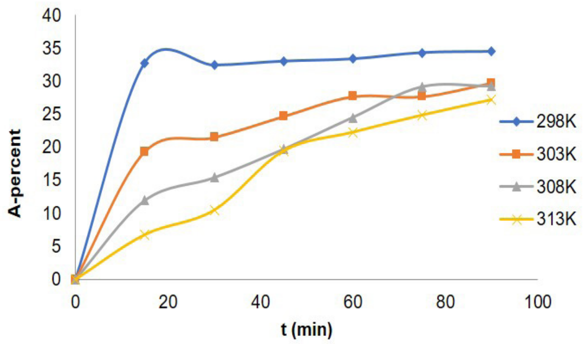

Fig. 4. Effect of contact time on the adsorption of JG dye onto ABP surface at different temperatures

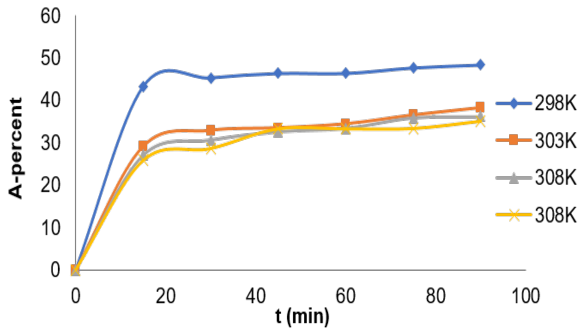

Fig. 5. Effect of contact time on the adsorption of JG dye onto MABP surface at different temperatures

Kinetic study for adsorption: The first-order and second-order kinetic models were applied to the experimental data and their kinetic parameters are presented in Table 1 and 2. The linear form of this model equation is given as (Lagergren).

$$Ln(q_e - q_t) = Lnq_e - k_1 t \quad (4)$$

k_1 - the Lagergren rate constant of adsorption (min^{-1})
q_e and q_t - the quantities of JG dye adsorbed (mg/g) at (t_e and t_t), respectively.

The slope and intercept of the plots of ln (q_e-q_t) versus t were used to determine the first-order rate constant k_l and the equilibrium adsorption capacity q_e for JG dye. The linear form of the second order equation is expressed as:

$$\frac{1}{q_t} = \frac{1}{k_2 q_e^2} + \frac{t}{q_e} \quad \textbf{(5)}$$

k_2 (g/mg.min) - the equilibrium constant of pseudo second order adsorption [26].

Table 1. First order and second order kinetics data for adsorption of JG dye on ABP surface

T/K	ABP		
	First order		
	k_1 (g mg^{-1} min^{-1})	q_e(mg/g)(cal)	R^2
298	0.035	2.990	0.66
303	0.031	11.485	0.929
308	0.078	81.557	0.710
313	0.0371	26.115	0.974
	Second order		
T/K	k_2 (g mg^{-1} min^{-1})	q_e(mg/g)(cal)	R^2
298	0.022	21.882	0.999
303	0.003	21.142	0.992
308	0.001	29.412	0.930
313	0.0001	51.813	0.654

Table 2. First and second order kinetics data for adsorption of JG dye on MABP surface

T/K	MABP		
	First order		
	k_1 (g mg^{-1} min^{-1})	q_e(mg/g)(cal)	R^2
298	0.029	4.945	0.903
303	0.025	8.133	0.917
308	0.052	17.179	0.809
313	0.031	8.064	0.809
	Second order		
T/K	k_2 (g mg^{-1} min^{-1})	q_e(mg/g)(cal)	R^2
298	0.012	30.864	0.999
303	0.005	25.189	0.995
308	0.005	24.450	0.998
313	0.006	23.529	0.997

It is noted from the Tables (1 and 2) that the R^2 values of the second-order model for the practical data of JG dye adsorption by the two surfaces (ABP and MABP) are higher than the R^2 values of the first-order model for most temperature. In addition to the convergence between the practical and theoretical value of the adsorption amount according to the second-order kinetic model being higher than according to the first-order. This leads to the fact that the kinetic data for the JG dye adsorption process on both surfaces follows the second-order kinetic model, which means that chemical adsorption is dominant in the process of JG dye adsorption on both surfaces [27].

Isothermal and thermodynamic study for JG dye adsorption: Equilibrium adsorption isotherms provide useful information for designing and optimizing operating procedures for adsorption systems at equilibrium. The Langmuir and Freundlich isotherm models were applied to the practical data and their parameters are given in Tables 3, 4. The Langmuir isotherm model can be expressed as the following equation:

$$\frac{C_e}{q_e} = \frac{1}{q_m . k_L} + \frac{C_e}{q_m} \quad \textbf{(6)}$$

q_L (mg/g) and k_L (L/mg)-the monolayer adsorption capacity of surfaces (ABP, MABP) and the Langmuir affinity parameter respectively. The constants q_L and k_L were calculated from the slope and intercept of the linear plot of c_e / q_e versus c_e. The linear form of Freundlich isotherm can be represented as:

$$Lnq_e = Lnk_F + \frac{1}{n} LnC_e \quad \textbf{(7)}$$

k_F is the Freundlich constant related to the adsorption capacity (mg/g), and n a constant related to the adsorption intensity of the adsorbent (L/mg). Therefore, the plot of lnq_e versus LnC_e gives a straight line of slope 1/n and intercepts lnk_F [28].

It is noted from the Tables 3, 4 that the R^2 values of the Freundlich isotherm equation for the practical data of dye adsorption by the two surfaces are greater than the R^2 values of the Langmuir isotherm equation for all temperatures. Also the value of the Freundlich constant (k_F) for the composite (MABP) is greater than it is for the original surface (ABP) for all temperatures, which indicates that the adsorption process tends to favor the complex to a greater degree than it does for the original surface. Also notice that the values (n< and >1) when the temperature increases, which indicates that the type of adsorption changes from physical-chemical adsorption to chemical adsorption due to the effect of temperature on both surfaces. This leads to that the equilibrium data for the dye adsorption process on both surfaces follow the Freundlich isotherm model, which means that the surfaces (ABP and MABP) are of heterogeneous nature and that the JG adsorption may be single or multilayer [29]. Thermodynamic parameters, including changes in Gibbs free energy (ΔG), changes in enthalpy (ΔH), changes in entropy (ΔS), and equilibrium constant (k_{eq}) for the adsorption process were calculated using the following equations:

$$k_{eq} = \frac{q_e . V}{C_e . m} \quad \textbf{(8)}$$

$$\Delta G^\circ = -RTLnk_{eq} \quad \textbf{(9)}$$

Table 3. The calculated constants and correlation coefficients (R^2) for Langmuir isotherm of JG dye adsorption onto ABP and MABP surfaces

T/K	ABP			MABP		
	k_L	q_m	R^2	k_L	q_m	R^2
298	0.064	36.900	0.830	0.066	98.039	0.725
303	0.045	30.030	0.834	0.002	1428.571	0.011
308	0.018	42.553	0.628	-0.018	-117.647	0.216
313	-0.006	-67.114	0.124	-0.026	-62.112	0.356

Table 4. The calculated constants and correlation coefficients (R^2) for Freundlich isotherm of JG dye onto ABP and MABP surfaces

T/K	ABP			MABP		
	k_F	n	R^2	k_F	n	R^2
298	4.587	2.011	0.879	8.163	1.492	0.920
303	2.467	1.721	0.912	2.979	0.981	0.959
308	1.132	1.301	0.952	1.401	0.782	0.915
313	0.307	0.877	0.926	0.835	0.692	0.907

Table 5. The thermodynamic parameters for the adsorption of JG dye onto ABP and MABP surfaces

T/K	ABP			MABP		
	ΔG (J/mol)	ΔH (J/mol)	ΔS (J/mol.K)	ΔG (J/mol)	ΔH (J/mol)	ΔS (J/mol.K)
298	-2140.4	-39287.0	-124.7	-4986.374	-11895.671	-23.186
303	-979.6		-126.4	-4846.084		-23.266
308	-509.2		-125.9	-4705.615		-23.344
313	-225.7		-124.8	-4647.672		-23.157

$$Lnk_{eq} = -\frac{\Delta H^{\circ}}{RT} + cons\tan t \quad (10)$$

$$\Delta G^{\circ} = \Delta H^{\circ} - T\Delta S^{\circ} \quad (11)$$

T - the temperature (K)
R the ideal gas constant (8.314 J/mol .K)
k_{eq} - the thermodynamic equilibrium constant [30].

It is noted from Table 5 that the values of (ΔG) are negative, which indicates the spontaneity of the JG dye adsorption process, which decreases with increasing temperature, and this is more so on the modified surface than on the activated surface. The values of (ΔH) are negative, which indicates that the nature of adsorption is exothermic, and the negative values of (ΔS) do not indicate that the process of adsorption of JG dye molecules is regular at low temperatures and the degree of uniformity becomes fluctuating as the temperature increases [31,32].

CONCLUSIONS

The processes of thermal activation of banana peels (ABP) and the formation of a nanocomposite with iron oxide nanoparticles (MABP) have been proven successful through two techniques (XRD and FT-IR). The surfaces were tested in the process of adsorption of JG dye with an efficiency of up to 33% and 46% for both surfaces (ABP and MABP) respectively. Kinetically, it was found that the adsorption process follows the second-order kinetic model, which indicates the type of chemical adsorption, while the equilibrium data followed the Freundlich isotherm model, which indicates that the adsorbent surfaces are of a heterogeneous nature. The negative values of the thermodynamic functions refer to the adsorption process is spontaneous, regular, and exothermic nature.

ACKNOWLEDGEMENT

We thank the Department of Chemistry at the College of Education for Pure Sciences, Ibn al-Haitham, within the University of Baghdad for supporting us with the tools, materials, and laboratories to complete this work, with appreciation and gratitude.

REFERENCES

1. Maimuna A., Fahim B.A.R., Zainal Abedin M., Fijul Kabir S.M. (2021). Adsorption characteristics of banana peel in the removal of dyes from textile effluent. *Textiles*, **1**, 361-375. https://doi.org/10.3390/textiles1020018
2. Wong S., Abd Ghafar N., Ngadi N., Razmi F.A., Inuwa I.M., *et al*. (2020). Effective removal of anionic textile dyes using adsorbent synthesized from coffee waste. *Sci. Rep*., **10**, 1-13. https://doi.org/10.1038/s41598-020-60021-6
3. Bodini A., Chiussi S., Donati M., Bellassen V., Török Á., *et al*. (2021). Water footprint of food quality schemes. *J. Agric. Food Ind. Organ*., **19**(2), 145-160. https://doi.org/10.1515/jafio-2019-0045
4. Akpor O.B., Muchie M. (2011). Environmental and public health implications of wastewater quality. *Afr. J. Biotechnol*., **10**(13), 2379-2387. https://doi.org/10.5897/AJB10.1797
5. Ziarani G.M., Moradi R., Lashgari N., Kruger H.G. (2018). Introduction and importance of synthetic organic dyes. In: Metal-free synthetic organic dyes. Elsevier, 1-7. https://doi.org/10.1016/C2017-0-03672-8
6. Bhatia D., Sharma N.R., Singh J., Kanwar R.S. (2017). Biological methods for textile dye removal from wastewater: A review. *Crit. Rev. Environ. Sci. Technol*., **47**(19), 1836-1876. https://doi.org/10.1080/10643389.2017.1393263
7. Nahiun K.M., Bijoyee S., Kamrun N.K., Fatin I.M., Shahirin S., *et al*. (2021). A review on the methods of industrial waste water treatment. *Scientific Review*, **7**(3), 20-31. https://doi.org/10.32861/sr.73.20.31
8. Naushad M., Ahamad T., Alothman Z. A., Ala'a H. (2019). Green and eco-friendly nanocomposite for the removal of toxic Hg (II) metal ion from aqueous environment: Adsorption kinetics & isotherm modelling. *J. Mol. Liq*., **279**, 1-8. https://doi.org/10.1016/j.molliq.2019.01.090
9. Arami M., Limaee N.Y., Mahmoodi N.M., Tabrizi N.S. (2005). Removal of dyes from colored textile wastewater by orange peel adsorbent: Equilibrium and kinetic studies. *J. Colloid Interface Sci*., **288**, 371-376. https://doi.org/10.1016/j.jcis.2005.03.020
10. Munagapati V.S., Wen J.C., Pan C.L., Gutha Y., Wen J.H., *et al*. (2020). Adsorptive removal of anionic dye (Reactive Black 5) from aqueoussolution using chemically modified banana peel powder: Kinetic, isotherm, thermodynamic, and reusability studies. *Int. J. Phytoremediation*, **22**, 267-278. https://doi.org/10.1080/15226514.2019.1658709
11. Kyzas G.Z., Matis K.A. (2015). Nanoadsorbents for pollutants removal: A review. *J. Mol. Liq.,* **203**, 159-168. https://doi.org/10.1016/j.molliq.2015.01.004
12. Modrogan C., Capr arescu S.D., Ancil A.M., Orbule O.D., Vasile E., *et al*. (2020). Mixed oxide layered double hydroxide materials: Synthesis, characterization and efficient application for Mn^{2+} removal from synthetic wastewater. *Materials*, **13**, 4089. https://doi.org/10.3390/ma13184089
13. Haider A.J.A., Ahmed H.A.A., Saad A.A., Raghad S.M. (2023). Microbial simultaneous eradication from wastewater of sulphate and heavy metals. *As. J. Water, Environ. Pollut*., **20**(3), 85-90. https://doi.org/10.3233/AJW230041
14. Kamar F.H., Niamat F.E., Faisal A.A., Mohammed A.A., Nechifor A.C., *et al*. (2018). Use of artificial neural network for modeling and prediction of reactive red dye removal from wastewater using banana peels bio-sorbent. *Rev. De Chim*., **69**, 1919-1926. https://doi.org/10.37358/RC.18.8.6447
15. Oyekanmi A.A., Ahmad A., Hossain K., Rafatullah M. (2019). Adsorption of Rhodamine B dye from aqueous solution onto acid treated banana peel: Response surface methodology, kinetics and isotherm studies. *PLoS ONE*, 14, e0216878. https://doi.org/10.1371/journal.pone.0216878
16. Ma J., Huang D., Zou J., Li L., Kong Y., Komarneni S. (2015). Adsorption of methylene blue and Orange II pollutants on activated carbon Mondal N.K., Kar S. (2018). Potentiality of banana peel for removal of Congo red dye from aqueous solution: Isotherm, kinetics and thermodynamics studies. *Appl. Water Sci*., **8**, 157. https://doi.org/10.1007/s13201-018-0811-x
17. Amr H.H., Ebrahim S., Mohamed S.H. (2020). Green and ecofriendly bio-removal of methylene blue dye from aqueous solution using biologically activated banana peel waste. *Sustain. Chem. Pharm.,* **18**, 100333. https://doi.org/10.1016/j.scp.2020.100333
18. Abd S.S., Abbas A.M. (2019). Preparation, characterization and adsorption capacity of bauxite-carbon nanotube composite. *Nat. Environ.and Poll. Technol*., **18**(3), 863-869. https://www.neptjournal.com/upload-images/NL-69-20-(18)-D-875.pdf
19. Khairiah K., Erna F., Kerista S., Perdinan S., Syahrul H. (2021). Data on characterization, model, and adsorption rate of banana peel activated carbon (Musa Acuminata) for adsorbents of various heavy metals (Mn, Pb, Zn, Fe). *Data in Brief*, **39**, 1-9. https://doi.org/10.1016/j.dib.2021.107611
20. Abhijeet M., Meryam S. (2014). Isolation of genomic DNA by silane-modified iron oxide nanoparticles. In: Bhupinder S., Anupama K., Mehta S.K, Tripathi S.K. (eds) Nanotechnology, McGraw Hill, **45**, 308-315.
21. Muntaka D., Zakariyya U.Z., Maje A.H. (2018). Cationic dyes removal using low-cost banana peel biosorbent. *Am. J. Mater. Sci.,* **8**(2), 32-38. https://doi.org/10.5923/j.materials.20180802.02
22. Khalil M.I. (2015). Co-precipitation in aqueous solution synthesis of magnetite nanoparticles using iron (III) salts as precursors. *Arab. J. Chem.,* **8**, 279-284.

https://doi.org/10.1016/j.arabjc.2015.02.008

23. Fatemeh G.M.M., Bahri R.A. (2018). Adsorption of Cr (VI) from aqueous solution by adsorbent prepared from paper mill sludge: Kinetics and thermodynamics studies. *Adsorp. Sci. Tech.*, **36**(1-2), 149-169. https://doi.org/10.1177/0263617416686976
24. Abbas J.S., Ahmed M.A. (2023). Kinetic study for janus green dye adsorption from aqueous solutions using iraqi bauxite clay and its composite. *Wasit J. Pure Sci.*, **2**(1), 42-52. https://doi.org/10.31185/wjps.116
25. Kazem M.S., Abbas A.M. (2022). Study of inorganic doping of kaolin clay, a kinetic study of adsorption of methyl green dye from its aqueous solutions. *Eurasian Chem. Commun.*, **4**(12), 1218-1227. https://doi.org/10.22034/ecc.2022.342243.1467
26. Faraj R.A.S., Abbas A.M. (2021). Loading and activating a carbon surface and applied for congo red adsorption, kinetic study. *Journal of Physics: Conference Series,* **1879**(2), 022076-022090. https://doi.org/10.1088/1742-6596/1879/2/022076
27. Jasim M.A., Abbas A.M., Radhi I.M. (2021). Preparation and characterization of biomass-alumina composite as adsorbent for safranine-o dye from aqueous solution at different temperatures. *AIP Conf. Proc.*, **2372**, 120001-120017. https://doi.org/10.1063/5.0068746
28. Jasim M.A., Abbas A.M. (2019). Equilibrium and thermodynamic study of malachite green & phenol red dyes adsorption from aqueous solution by use algae biomass. *J. Global Pharma Technol.*, **11**(2), 21-31. https://doi.org/10.4028/www.scientific.net/AMM.148-149.470
29. Osich J., Cooper L. (1982) Adsorption. *John Wiley and Sons*. New-York, 126.
30. Majida H.O. (2011). Thermodynamic study of adsorption cationic methylene blue dye on the plant residue. *Journal of Kufa for Chemical Science,* (**2**), 55-63. https://journal.uokufa.edu.iq/index.php/jkcs/article/view/3459
31. Ahmed M.A., Firas H.A., Walaa J.S., Rusul A.S.F. (2020). Adsorption of dyes by activated carbon surfaces were prepared from plant residues, A Review. *J. Mater. Environ. Sci.,* **11**(12), 2007-2015. https://www.jmaterenvironsci.com/Document/vol11/vol11_N12/JMES-2020-11171-Abbas.pdf